MRS Communications

https://doi.org/10.1557/s43579-025-00835-5

MRS Communications

Research Letter

Printing orientation effects on microstructure in LPBF-manufactured SS316L subjected to fatigue

Mateusz Kopec, Institute of Fundamental Technological Research, Polish Academy of Sciences, Pawińskiego 5B, 02-106 Warsaw, Poland; Institute for Innovation in Sustainable Engineering, College of Engineering and Technology, University of Derby, Derby DE1 3HD, UK
Dominika Przygucka, Faculty of Advanced Technologies and Chemistry, Military University of Technology, 00-908 Warsaw, Poland
Marzena Pawlik, and Paul Wood, Institute for Innovation in Sustainable Engineering, College of Engineering and Technology, University of Derby, Derby DE1 3HD, UK
Stanisław Jóźwiak, Faculty of Advanced Technologies and Chemistry, Military University of Technology, 00-908 Warsaw, Poland
Zbigniew L. Kowalewski, Institute of Fundamental Technological Research, Polish Academy of Sciences, Pawińskiego 5B, 02-106 Warsaw, Poland

Address all correspondence to Mateusz Kopec at **mkopec@ippt.pan.pl**

(Received 4 May 2025; accepted 12 September 2025)

Abstract

In this paper, printing orientation effects on the microstructure and fatigue behavior of SS316L produced *via* Laser Powder Bed Fusion (LPBF) were studied. Specimens printed in Z (vertical), XY (horizontal), and ZX (45°) orientations were subjected to cyclic loading in the range from ± 300 to ± 500 MPa. EBSD analysis revealed that XY-oriented samples had superior fatigue resistance due to low-angle grain boundaries, while Z-oriented samples showed increased high-angle grain boundaries, leading to early crack initiation.

Introduction

The advancement of additive manufacturing (AM) has revolutionized the production of metallic components by enabling the fabrication of complex geometries with high precision and minimal material waste.[1] Among AM techniques, LPBF has emerged as a widely adopted method for manufacturing stainless steel components due to its ability to produce high-density structures with tailored mechanical properties.[2] Stainless steel 316L is particularly suitable for applications in aerospace, biomedical, and structural engineering, where mechanical performance, including fatigue resistance, plays a crucial role in component longevity and reliability.[3]

One of the primary challenges associated with LPBF-manufactured components is the microstructural anisotropy caused by layer-by-layer deposition.[4] The thermal history, including rapid cooling rates and localized heating, leads to the formation of columnar grains, residual stresses, and variations in grain boundary misorientation depending on the build direction.[5] These microstructural characteristics significantly impact mechanical behavior, particularly in fatigue loading conditions. Given that LPBF-produced parts often operate in environments where fatigue failure is a concern, understanding the relationship between printing orientation, microstructural evolution, and fatigue performance is essential.[6]

Despite extensive research on the mechanical properties of LPBF-processed SS316L, a comprehensive study linking printing orientation to microstructural changes and ultimately to fatigue response is still limited. Existing studies primarily focused on analysis of printing orientation and surface roughness on fatigue performance.[7] However, misorientation angle values for different printing orientation before and after the deformation were not reported. More recently, Lyu et al.[8] investigated one printing direction and the role of low-angle grain boundaries (LAGB) and high-angle grain boundaries (HAGB) on high-cycle fatigue of LPBF-manufactured SS316L considering the role of lack of fusion defects, grains, and dislocation cells. In the HCF regime, the orientation of the grain was mainly maintained, and an increase in-grain misorientation due to the relatively small plastic deformation was observed. The effect of printing orientation on fatigue resistance, grain boundary characteristics, and phase transformations remains an area of ongoing investigation. The anisotropic nature of the LPBF process results in distinct grain structures in the Z (vertical), XY (horizontal), and ZX (45°) orientations, leading to variations in fatigue resistance due to differences in crack initiation and propagation behavior.

Therefore, in this study, the systematical analysis of the printing orientation effects on the microstructure and fatigue behavior of LPBF-manufactured SS316L was performed. Using Electron Backscatter Diffraction (EBSD) analysis, misorientation angle measurements, and grain boundary mapping, a correlation between microstructural evolution and fatigue response was established. Fatigue tests conducted at different stress amplitudes ranging from ± 300 MPa to ± 500 MPa provide insight into the deformation mechanisms and failure modes associated with different build directions. By examining the microstructural transformations in deformed and non-deformed specimens, the research aims to provide a better understanding of how printing parameters influence fatigue life and grain boundary stability in LPBF-processed SS316L.

Materials and methods

Renishaw provided the initial SS316L powder feedstock. After being processed through the LPBF technique, any remaining SS316L powder that was not utilized was collected and sieved using a Russell Finex sieve (model MS400) with a 63 µm mesh. This sieving process was performed to remove fine satellite particles and oxides before reusing the powder. Each LPBF process followed the default print settings assigned by the Renishaw Quant AM software, which were linked to the input CAD model. The reused powder had undergone 25 reuse cycles over multiple years within the powder bed, with occasional replenishment using small amounts of fresh powder.[9] Generally, the proportion of fresh powder added remained below 2% to maintain the necessary powder bed volume.

The additive manufacturing process was carried out using the Renishaw AM 250 system, which utilized a 200 W laser, a 70 µm spot size, and a 1070 nm wavelength, following the parameters detailed in Fig. 1(a). Specimens of cylindrical (10 mm diameter, 56 mm length) shapes were fabricated in three orientations relative to the build plate: Z (vertical), XY (horizontal), and ZX (45°), as depicted in Fig. 1(b).

Following fabrication, the specimens underwent stress relief heat treatment, involving soaking at 470℃ for six hours while still attached to the build plate. Once heat treatment was completed, the specimens were separated from the build

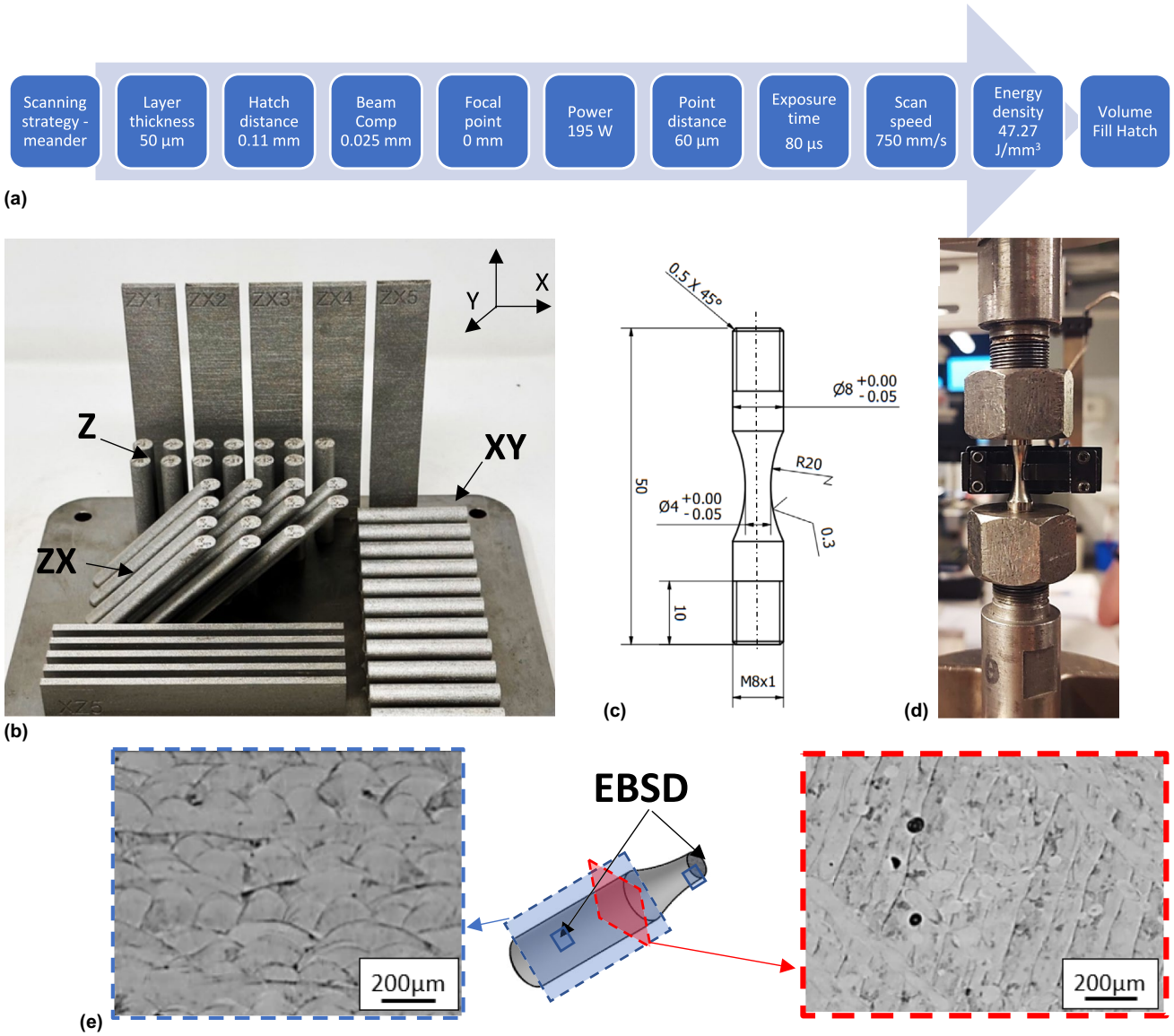

Figure 1. Process parameters applied during AM (a); printing orientations of the SS316L bars (b); engineering drawing of the hourglass specimen (c); general view of the assembled specimen during fatigue testing (d); schematic drawing of fractured specimen after fatigue testing with exposed view of EBSD region of interest and two cross-sections in which microstructure of the as-built alloy was shown in parallel and perpendicular directions with respect to that of the building section (e).

plate through Electrical Discharge Machining (EDM) using a wire cut system (AgieCharmilles Cut E 350). The wire diameter ranged from 0.1 mm to 0.3 mm, and the cutting process achieved axis speeds of up to 3000 mm/min. Additional machining was conducted using a Haas Automation ST-20Y lathe to achieve the geometry presented in Fig. 1(c).

To ensure that the residual microstructure accurately reflected the volume fill hatch scanning parameters, more than 2 mm of material was removed from the gauge section of the fatigue samples. This step was necessary to eliminate the influence of the border scan zone, where higher laser energy density affected the surface and subsurface layers, allowing for an isolated evaluation of microstructural characteristics in the volume fill hatch region. Figure 2(d) provides an overall view of the specimen fixed in the testing machine grip.

Uniaxial tensile testing was performed with respect to ASTM Standard E8/8 M at a strain rate of 0.001/s using an MTS 858 machine equipped with a 250 kN load cell to determine key material properties, including conventional yield strength (YS). The range of stress amplitude was determined based on the YS value. To enhance the reliability of the results, three uniaxial tensile tests were carried out for each sample orientation.

The fatigue test was performed with respect to ASTM Standard E606. The MTS 858 machine operated under force control, maintaining a zero mean stress level and applying a constant stress amplitude between ± 300 MPa and ± 500 MPa at a frequency of 20 Hz. A transverse MTS extensometer was used to measure diameter variations throughout the test. Axial strain calculations were conducted using a Poisson's ratio of 0.33. Each stress amplitude condition was tested using three specimens to ensure consistency in results.

Samples for microstructural analysis were extracted from both the deformed region near the fracture surface (approx. 1 mm from fracture) and the non-deformed section from the specimen grip, as illustrated in Fig. 1(e). These samples were embedded in conductive resin before undergoing a polishing process, which included a 1 μm diamond surface finish and a 1200-grit Bakelite diamond grinding wheel. After polishing, the samples were etched with an electrolytic oxalic acid solution for 5 to 15 s. EBSD analysis was performed using a high-resolution Quanta 3D FEG scanning electron microscope operating at an acceleration voltage of 20 kV.

Experimental results and discussion

The tensile tests revealed notable variations in mechanical properties based on build orientation [Fig. 2(a)]. The XY-oriented specimens exhibited the highest ultimate tensile strength (R_m = 763 MPa) and yield strength (R_e = 596 MPa), along with a significant elongation of 45.9%. In contrast, the Z-oriented specimens showed the lowest strength values (R_m = 700 MPa, R_e = 524 MPa), with an intermediate elongation of 38.8%. The ZX specimens exhibited a tensile strength of 740 MPa and yield strength of 549 MPa, with an elongation of 29.5%. These differences were attributed to the microstructural anisotropy introduced by the layer-by-layer deposition process, which influences grain growth and defect distribution.[10] Fatigue testing was carried out to assess the cyclic loading performance of the LPBF-manufactured SS316L specimens [Fig. 2(b)]. The cylindrical fatigue specimens were printed in Z, XY, and ZX orientations and subjected to cyclic loading at different stress amplitudes. The results showed a clear dependence of fatigue behavior on printing orientation. The XY-oriented specimens exhibited superior fatigue performance, with a longer fatigue life compared to the Z and ZX orientations. The Z-oriented specimens demonstrated the lowest fatigue resistance, which can be linked to the presence of columnar grains aligned parallel to the build direction, making them more susceptible to crack initiation and propagation under cyclic loading.[8]

The fatigue behavior of LPBF-manufactured SS316L exhibited a strong dependence on build orientation and applied stress amplitude. At a lower stress amplitude of ± 300 MPa, the microstructure remained relatively stable across all orientations, with only minor changes in misorientation angles (Fig. 3). The XY-oriented specimens, characterized by equiaxed

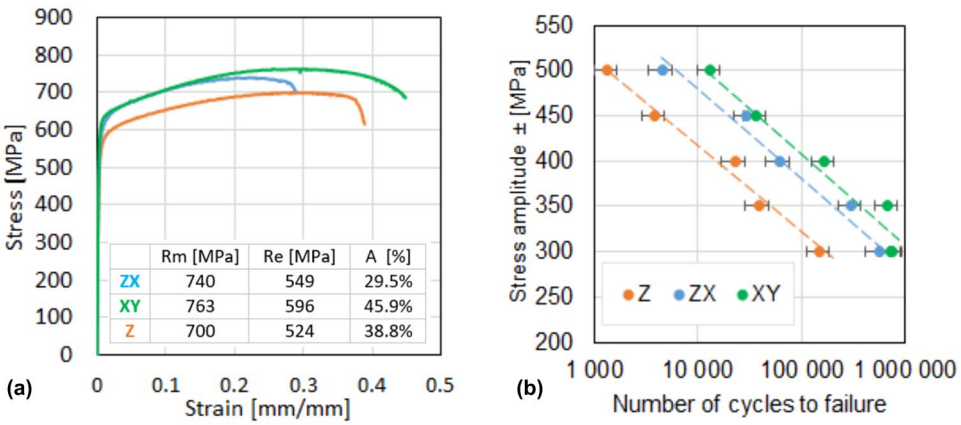

Figure 2. Stress–strain (a) and S–N (b) characteristics of the LPBF-manufactured SS316L printed in different orientations.

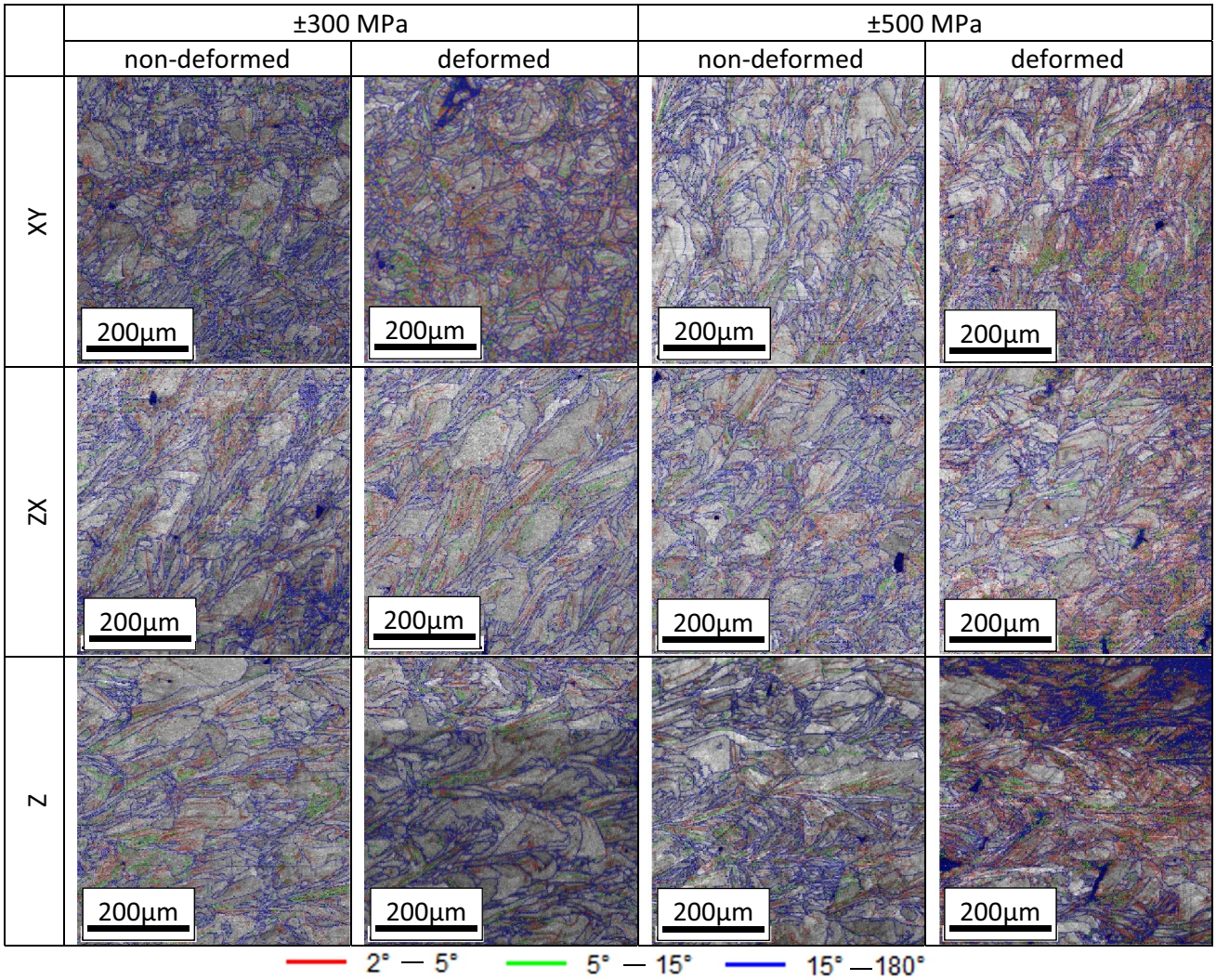

Figure 3. Grain boundaries maps of SS316L specimens manufactured at XY, ZX, and Z direction and tested at the stress amplitude equal to ± 300 MPa and ± 500 MPa.

grains, displayed the highest fatigue resistance. Such microstructure enabled for a uniform distribution of cyclic stresses, resulting in strain localization reduction and crack initiation delay.[11] In contrast, Z-oriented specimens, composed predominantly of columnar grains aligned parallel to the build direction, exhibited earlier fatigue damage initiation. Cyclic loading along the grain direction promoted intergranular crack formation and slip band activity, making these specimens more susceptible to fatigue failure.[12] The ZX-oriented samples, of a mixed microstructure of both columnar and equiaxed grains, exhibited intermediate fatigue resistance, with some signs of strain accumulation but less severe damage compared to Z-oriented specimens. At a higher stress amplitude of ± 500 MPa, significant microstructural degradation was observed in all specimens. The Z-oriented specimens experienced the most pronounced grain boundary evolution, with a sharp increase in HAGBs and evidence of grain fragmentation. The cyclic plasticity induced by high-stress fatigue loading caused grain rotation and misorientation changes, leading to localized strain accumulation and accelerating crack initiation.[13] The XY-oriented specimens, while also exhibiting increased grain misorientation, retained a higher fraction of LAGBs, which distribute stress more evenly and delayed fatigue failure.[14] The ZX-oriented specimens again showed an intermediate response, with both HAGB and LAGB fractions increasing due to strain-induced grain boundary migration and localized grain fragmentation. The proportions of LAGBs (2°–15°) and HAGBs (15°–180°) were quantitatively assessed based on the normalized misorientation data. In the non-deformed condition at ± 300 MPa, the XY-oriented specimens exhibited a predominantly HAGB-rich structure (70.4%), with LAGBs comprising approximately 19.4% of the boundaries, whereas the Z-oriented specimens showed a slightly lower initial HAGB fraction (60.8%) and a higher LAGB content (39.3%), indicating a

greater presence of columnar grains with internal misorientations. Under stress amplitude of ± 500 MPa, all orientations experienced an increase in LAGBs and subsequent reduction in HAGBs, consistent with grain fragmentation and rotation mechanisms. Notably, the Z-oriented specimens exhibited the highest post-deformation HAGB content (51.4%) and the largest increase in LAGBs (from 39.3 to 48.6%). In contrast, the XY-oriented specimens retained a HAGB fraction of 44.2% and LAGBs of 55.8%, reflecting a more uniform deformation mode that correlates with their superior fatigue resistance. The ZX orientation displayed intermediate behavior, both in terms of boundary evolution and mechanical performance. It was observed that a higher retained fraction of LAGBs in the XY orientation contributes to more effective dislocation absorption and strain accommodation, thereby delaying crack initiation, while the accumulation of HAGBs in the Z orientation under cyclic loading enhances local stress concentrations and promotes early failure.

Figure 4 illustrates the inverse pole figure (IPF) maps used to examine the texture development in SS316L components fabricated *via* laser powder bed fusion (LPBF). In the as-manufactured state without applied deformation, samples oriented along the Z-axis displayed a distinct crystallographic texture. This was characterized by columnar grains growing in alignment with the build direction, predominantly following ⟨001⟩ or ⟨101⟩ orientations. Such texture formation is a direct result of directional solidification, driven by steep thermal gradients during the LPBF process. In contrast, samples oriented in the XY-plane showed a more randomized texture, featuring mostly equiaxed grains—indicative of a more uniform and isotropic microstructure. For specimens printed at a 45° angle (ZX orientation), the microstructure reflected a mix of both equiaxed and columnar grains, suggesting a transitional texture between the Z and XY configurations. Following cyclic loading, especially under stress amplitudes of ± 500 MPa, the Z-oriented samples exhibited a noticeable reduction in texture intensity. The IPF maps indicated a wider and less defined spread of grain orientations, implying significant grain rotation, increased misorientations, and pronounced plastic deformation. These findings correspond well with the observed rise in high-angle grain boundaries (HAGBs) and the signs of grain fragmentation visible in the grain boundary and misorientation maps. Conversely, the XY-oriented samples largely retained their equiaxed grain structure, even under severe loading. This stability suggests that the grains deform more evenly under cyclic stress, thereby limiting localized strain accumulation and contributing to improved fatigue resistance. The ZX-oriented specimens showed intermediate behavior, with moderate texture changes, consistent with their mixed microstructure and fatigue response.

One should highlight, that in LPBF-manufactured SS316L, fatigue performance is strongly influenced by a initial microstructure and process parameters. The build orientation significantly affects grain morphology and anisotropy. Since Z-oriented specimens exhibiting columnar grains aligned along the build direction, their fatigue resistance due to easier crack propagation was the lowest. On the contrary, XY-oriented specimens, characterized by equiaxed and more uniformly distributed grains, show superior fatigue performance, while ZX-ones characterized by intermediate behavior due to their mixed grain structure. It should be stressed that fatigue loading under high amplitude of ± 500 MPa increases HAGBs. It promotes localized strain accumulation and early crack initiation. On the other hand, a higher fraction of LAGBs, as seen in XY builds, distribute strain more evenly and thus delay failure. Additionally, residual stresses commonly found after the LPBF process also contribute to fatigue damage. It should be mentioned, that post-process heat treatment can relieve residual stresses and reduce dendritic cellular structures, thus enhancing fatigue resistance significantly.[15] Surface and subsurface defect distribution, influenced by laser energy density and hatch contour overlap, also impacts crack initiation, with low volumetric energy densities leading to more lack of fusion defects and higher defect complexity. Increasing energy density improves consolidation and fatigue performance, but even at high density, subsurface defects remain a limiting factor, especially in the high-cycle fatigue regime.[16,17]

Additionally, Kernel Average Misorientation (KAM) analysis was used to describe local plastic deformation, reflecting gradients in lattice rotation and dislocation density (Fig. 4). The KAM maps of LPBF-manufactured SS316L clearly demonstrate that cyclic loading induces progressive lattice curvature, with the most pronounced changes observed in Z-oriented specimens. The columnar grains aligned with the build direction facilitate slip localization along parallel crystallographic planes, leading to pronounced dislocation pile-up, intragranular misorientation, and grain rotation. The energy accumulated during cyclic loading is stored in crystal defects, predominantly dislocations, which are generated and glide within the active slip systems.[18] Upon becoming immobilized, these dislocations arrange into cellular structures. In the case of the Z-oriented specimens, the crystallographic orientation promotes the most intensive progression of this mechanism, resulting in a pronounced transformation of LAGBs into HAGBs and, consequently, the most substantial plastic deformation of the grains.[19] The enhanced HAGB fraction observed post-deformation corresponds to strain-induced grain fragmentation, which acts as preferential sites for crack initiation and accelerates fatigue failure. By contrast, XY-oriented specimens with equiaxed grain morphology exhibited a more homogeneous KAM distribution, indicating that plastic strain was accommodated in a more isotropic manner with lower strain gradients. This uniform strain distribution stabilizes the dislocation structure, delays the transition from LAGBs to HAGBs, and correlates with the superior fatigue resistance measured experimentally. The ZX specimens displayed intermediate behavior, consistent with their mixed texture and transitional mechanical response.

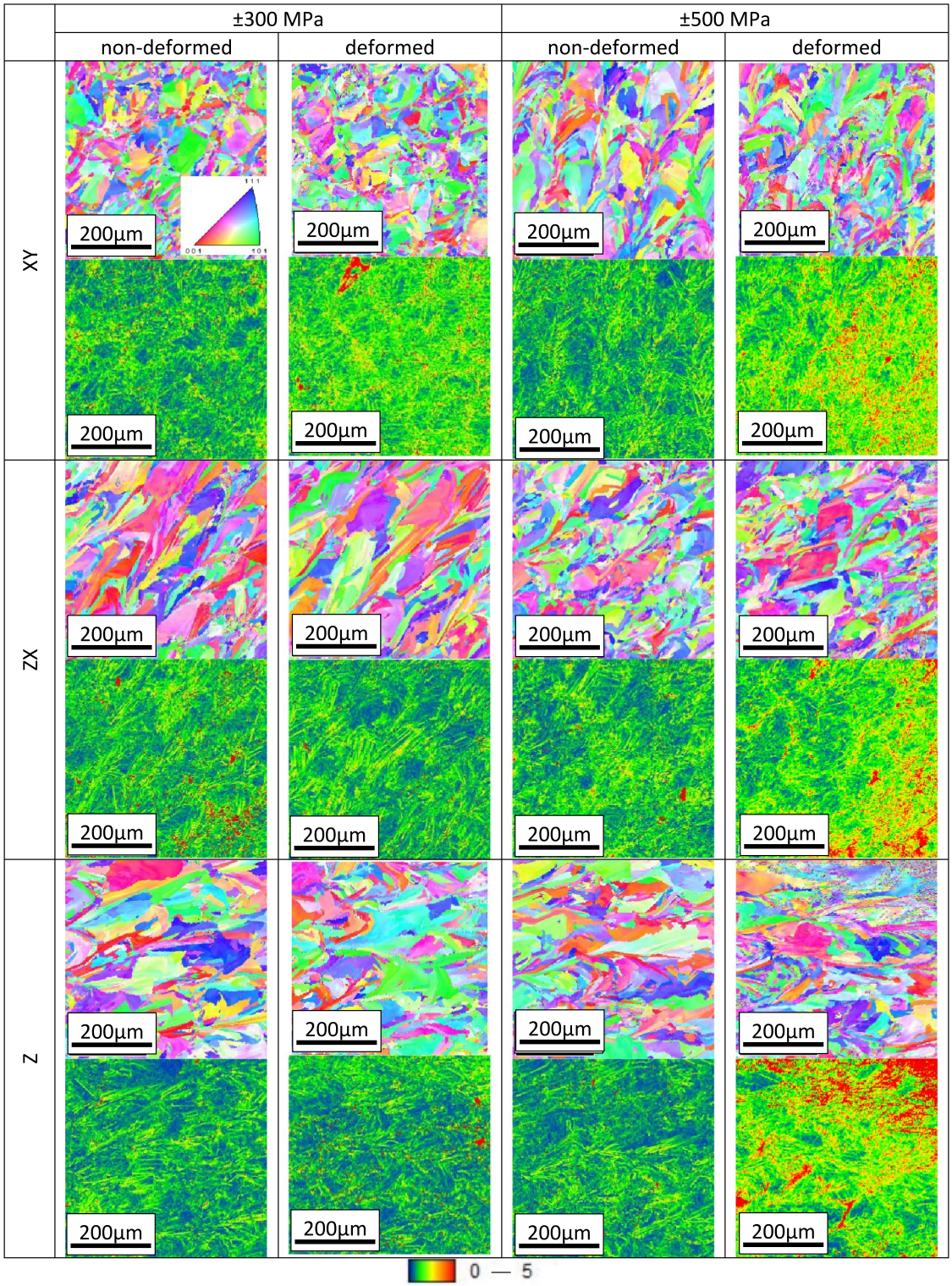

Figure 4. IPF and KAM maps of SS316L specimens manufactured at XY, ZX, and Z direction and tested at the stress amplitude equal to ± 300 MPa and ± 500 MPa.

Conclusions

The printing orientation has a significant impact on the fatigue performance of LPBF-manufactured SS316L. Specimens printed in the XY orientation exhibited the highest fatigue resistance, while those in the Z orientation showed the lowest due to the presence of columnar grains aligned with the build direction. The microstructural anisotropy resulting from the layer-by-layer fabrication process influenced crack initiation and propagation, with Z-oriented specimens being more susceptible to early failure. Under cyclic loading, HAGBs increased significantly in Z-oriented samples, leading to localized strain accumulation and grain fragmentation. In contrast, XY-oriented specimens maintained a more balanced grain boundary distribution, which helped delay fatigue failure. At higher stress amplitudes (±500 MPa), all specimens were characterized by grain rotation and misorientation changes, but the effect was most pronounced in the Z-oriented samples.

Acknowledgments

The authors would like to express their gratitude to Mr M. Wyszkowski for his kind help during the experimental part of this work.

Author contributions

Conceptualization: M.K.; Data curation: M.K., D.G., and S.J.; Formal analysis: M.K. and S.J.; Investigation: M.K., D.G., and P.W.; Methodology: M.K., S.J., Z.L.K., and P.W.; Project administration: M.K.; Supervision: M.K.; Validation: M.K., S.J., and P.W.; Visualization: M.K.; Roles/Writing—original draft: M.K.; and Writing—review & editing: M.K. and Z.L.K.

Funding

The research received no external funding.

Data availability

The data will be available on reasonable request.

Declarations

Conflict of interest

The authors declare they have no financial interests.

References

1. D. D'Andrea, Additive manufacturing of AISI 316L stainless steel: a review. Metals **13**(8), 1370 (2023)
2. J. Bedmar, A. Riquelme, P. Rodrigo, B. Torres, J. Rams, Comparison of different additive manufacturing methods for 316L stainless steel. Materials **14**(21), 6504 (2021)
3. M. Kopec, V.P. Dubey, M. Pawlik, P. Wood, Z.L. Kowalewski, Experimental identification of yield surface for additively manufactured stainless steel 316L under tension–compression-torsion conditions considering its printing orientation. Manuf. Lett. **41**, 28–32 (2024). https://doi.org/10.1016/j.mfglet.2024.07.003
4. W. Abd-Elaziem, S. Elkatatny, A.-E. Abd-Elaziem, M. Khedr, M.A. Abd El-baky, M.A. Hassan, M. Abu-Okail, M. Mohammed, A. Järvenpää, T. Allam, A. Hamada, On the current research progress of metallic materials fabricated by laser powder bed fusion process: a review. J. Mater. Res. Technol. **20**, 681–707 (2022). https://doi.org/10.1016/j.jmrt.2022.07.085
5. K. Deshmukh, A. Riensche, B. Bevans, R.J. Lane, K. Snyder, H.(Halliday, C.B. Williams, R. Mirzaeifar, P. Rao, Effect of processing parameters and thermal history on microstructure evolution and functional properties in laser powder bed fusion of 316L. Mater. Des. **244**, 113136 (2024). https://doi.org/10.1016/j.matdes.2024.113136
6. A. Avanzini, Fatigue behavior of additively manufactured stainless steel 316L. Materials **16**(1), 65 (2023)
7. W. Beard, R. Lancaster, N. Barnard, T. Jones, J. Adams, The influence of surface finish and build orientation on the low cycle fatigue behaviour of laser powder bed fused stainless steel 316L. Mater. Sci. Eng. A **864**, 144593 (2023). https://doi.org/10.1016/j.msea.2023.144593
8. X. Lyu, J. Zhang, F. Weber, A. Bezold, C. Broeckmann, Mechanical behaviours of the hierarchical microstructure of PBF-LB/M 316L SS during high cycle fatigue. Mater. Sci. Eng. A (2024). https://doi.org/10.1016/j.msea.2024.147652
9. M. Kopec, U. Gunputh, G. Williams, W. Macek, Z.L. Kowalewski, P. Wood, fatigue damage evolution in SS316L produced by powder bed fusion in different orientations with reused powder feedstock. Exp. Mech. (2024). https://doi.org/10.1007/s11340-024-01118-1
10. D. Kong, X. Ni, C. Dong, L. Zhang, C. Man, X. Cheng, X. Li, Anisotropy in the microstructure and mechanical property for the bulk and porous 316L stainless steel fabricated via selective laser melting. Mater. Lett. **235**, 1–5 (2019). https://doi.org/10.1016/j.matlet.2018.09.152
11. J.V. Gordon, C.V. Haden, H.F. Nied, R.P. Vinci, D.G. Harlow, Fatigue crack growth anisotropy, texture and residual stress in austenitic steel made by wire and arc additive manufacturing. Mater. Sci. Eng. A **724**, 431–438 (2018). https://doi.org/10.1016/j.msea.2018.03.075
12. P. Kumar, R. Jayaraj, J. Suryawanshi, U.R. Satwik, J. McKinnell, U. Ramamurty, Fatigue strength of additively manufactured 316L austenitic stainless steel. Acta Mater. **199**, 225–239 (2020). https://doi.org/10.1016/j.actamat.2020.08.033
13. G. Chai, A study on fatigue damage and crack initiation in austenitic steel matrix during very high cycle fatigue. Int. J. Fatigue **179**, 108033 (2024). https://doi.org/10.1016/j.ijfatigue.2023.108033
14. P. Wood, T. Libura, Z.L. Kowalewski, G. Williams, A. Serjouei, Influences of horizontal and vertical build orientations and post-fabrication processes on the fatigue behavior of stainless steel 316L produced by selective laser melting. Materials (2019). https://doi.org/10.3390/ma12244203
15. M. Winning, A.D. Rollett, Transition between low and high angle grain boundaries. Acta Mater. **53**(10), 2901–2907 (2005). https://doi.org/10.1016/j.actamat.2005.03.005
16. A. Hamada, M. Jaskari, T. Gundgire, A. Järvenpää, Enhancement and underlying fatigue mechanisms of laser powder bed fusion additive-manufactured 316L stainless steel. Mater. Sci. Eng. A **873**, 145021 (2023). https://doi.org/10.1016/j.msea.2023.145021
17. M. Jaskari, A. Hamada, T. Allam, K. Dzieciol, S. Ghosh, R. Schwaiger, P. Karjalainen, A. Järvenpää, Effects of volumetric energy density on defect structure

and fatigue behaviour of powder bed fusion manufactured 316L stainless steel. Mater. Sci. Eng. A **925**, 147868 (2025). https://doi.org/10.1016/j.msea.2025.147868
18. S.S.A. Shah, M. Liu, A. Khan, F. Ahmad, U.M. Chaudry, M.Y. Khan, M.R. Abdullah, S. Xu, Z. Peng, Recrystallization aspects and factors affecting their roles in Mg alloys: a comprehensive review. J. Magnes. Alloys. **13**(5), 1879–1914 (2025). https://doi.org/10.1016/j.jma.2025.03.020
19. M. Cao, Y. Liu, F.P.E. Dunne, A crystal plasticity approach to understand fatigue response with respect to pores in additive manufactured aluminium alloys. Int. J. Fatigue **161**, 106917 (2022). https://doi.org/10.1016/j.ijfatigue.2022.106917